Experimental study of surface segregation and wetting in films of a partially miscible polymer blend

M. Geoghegan,[1,*] R. A. L. Jones,[1] D. S. Sivia,[2] J. Penfold,[2] and A. S. Clough[3]
[1]*Cavendish Laboratory, University of Cambridge, Cambridge CB3 0HE, United Kingdom*
[2]*Rutherford Appleton Laboratory, Chilton, Didcot, Oxfordshire OX11 0QX, United Kingdom*
[3]*Department of Physics, University of Surrey, Guildford, Surrey GU2 5XH, United Kingdom*
(Received 17 August 1995)

We have studied composition-depth profiles in thin films of blends of deuterated polystyrene and poly(α-methyl styrene) using neutron reflectometry and ^{3}He nuclear reaction analysis. Some of the neutron reflectometry data are analyzed using a maximum entropy technique with Bayesian probability. One blend is miscible for all compositions at the temperature studied (180 °C), and we are able to obtain a bare surface energy difference between the two polymers from the equilibrium surface profile. The other blend that is studied is partially miscible, and here we have compared the approach to wetting in this blend with a simple model based on mean field theory. For quenches deeper into the metastable region of the phase diagram, the simple model fails due to, we believe, a competition between wetting and bulk nucleation and growth.

PACS number(s): 05.70.Fh, 36.20.−r, 47.20.Dr, 68.45.Gd

I. INTRODUCTION

There has been considerable experimental [1–18] and theoretical [3,19–34] interest of late in surface enrichment in thin polymer blend films. In a miscible blend, the surface is expected to be enriched, with respect to the bulk, in the component of lower surface energy; due to the large size of polymer molecules, these surface segregated layers can extend some distance into the bulk of the film. In a blend that is partially miscible in the bulk, alternate mechanisms of phase separation are available in thin films, and thick wetting layers of the lower surface energy component may grow [35]. Such phenomena are of great practical and theoretical interest as they represent a simple example of the behavior expected when phase transitions are influenced by confinement, reduced dimensionality, and surface effects. The theoretical starting point is still the mean field theory approach due to van der Waals [36–38]; in addition, the growing power of computers has facilitated complex Monte Carlo simulations of such phenomena [23,24,28,29]. This field may provide opportunities for improved coatings and for surface engineering of polymer based materials.

Quantitative data on surface segregation in miscible polymer blend films have been obtained in the past seven years. Miscible blends of polystyrene and poly(vinyl methyl ether) [1], and isotopic polystyrene (*d*-PS–*h*-PS) mixtures [2,3], showed significant surface enrichment of one component. In the latter case, the adsorbed amount was interpreted in terms of a mean field theory [22] and subsequently there has been a detailed examination of the shape of the near surface composition profile using neutron reflectometry (NR) [5]. These experiments were later extended to include a study of the kinetics of segregation [4,13].

There has been much less work on partially miscible polymer blend films quenched into the metastable region of the phase diagram, despite the theoretical interest that this has generated [10,15,23,24,27,31,34]. In such films a wetting layer will form and, in a semi-infinite system, grow indefinitely. Such growth is curtailed by finite size effects [21].

We choose to study blends of *d*-PS and poly(α-methyl styrene) (PαMS) as it is easy to access any part of the phase diagram and also because the phase diagram for these blends is well known, with good agreement as to the segmental interaction parameter using different experimental techniques [39–45]. One interesting difference between this system and previously studied systems is that the glass transition temperatures, and thus the segmental friction coefficients, are very different. This might be expected to lead to much more complicated kinetics than is observed in blends with components of comparable mobilities; we do indeed observe such complicated time dependent behavior.

In this paper we first describe determinations of the interaction parameter and then move on to a miscible blend. Here we consider the equilibrium configuration of the surface layer before moving on to discuss the kinetics of the segregation. We find that the equilibrium profile can be explained by mean field theory but with small discrepancies. However, the kinetics are not accounted for by simple ideas. Finally, we consider off-critical quenches inside the coexistence curve. We observe a wetting layer form and grow, and apply a simple model to the kinetics of the growth of the wetting layer. In order to understand our data we modify our model in an empirical way to account for the nucleation and growth of domains in the bulk of the film. For much of the reflectometry data discussed, we have used the relatively new maximum entropy method of analysis, the strengths and weaknesses of which we discuss below.

*Present address: Laboratoire Léon Brillouin, CE-Saclay, 91191 Gif-sur-Yvette Cedex, France.

II. EXPERIMENT

In all experiments we use *d*-PS with a molecular weight (MW) of 49 000 and two different PαMS chain lengths (MW 49 000 and 97 600). We shall refer to these blends as 49k-50k and 49k-97.6k, respectively. All polymers have polydispersity indices of 1.03 and were purchased from Polymer Laboratories. The films were spun cast from a toluene solution onto single crystal silicon wafers from which the native oxide layer had not been removed. The wafers were cleaned prior to casting by scrubbing with toluene and then methanol. The wafers were considered clean when the oxide layer was measured by ellipsometry to be less than 25 Å thick. The films were annealed in a vacuum oven at 180 °C [46] [the uncertainty in temperature is ±3 °C for NR samples, and ±1 °C for nuclear reaction analysis (NRA) samples]. The total film thickness was obtained using ellipsometry.

Neutron reflectometry [49,50] and ^{3}He nuclear reaction analysis [51] are ideal techniques for determining composition-depth profiles of polymer films, and we use them here. The NR experiments were performed on the CRISP reflectometer [49,52] of the ISIS spallation neutron source at the Rutherford Appelton Laboratory and the NRA experiments were performed at the Device Fabrication Facility at the University of Surrey. In NRA experiments a beam of ^{3}He ions is incident on the sample. The ions react with the deuterium present in the sample and produce high energy protons which are detected using a silicon barrier detector. The proton energy is dependent on the ^{3}He energy which therefore provides us with information on the depth in the film where the reaction took place. The *d*-PS composition-depth profile is determined by comparing the spectrum profile to that from a uniform *d*-PS film. The resolution of the experiment is limited compared to NR, but is much better at depth than other ion beam techniques such as forward recoil spectrometry. At Surrey, for a sample at 15° to the incident 700 keV beam a Gaussian resolution of width better than 140 Å is possible, staying reasonably constant with depth up to 4000 Å into the film. Recently, currents of better than 100 nA have been achieved and so the sample was left in the beam for only a few minutes to prevent significant beam damage and heating. The advantages and disadvantages of NR are well known and we will only briefly summarize them here. In NR experiments the reflectivity for values of the neutron wave vector, k (the perpendicular component of neutron momentum), above the critical value for total reflection is measured as a function of the wave vector. The reflectivity in the limit of large wave vectors is given by the modulus squared of the Fourier transform of the derivative of the scattering length density profile. Because of the loss of phase information, and because much of the experimental data fall outside the limit of validity of this approximation, reflectivity data cannot be directly inverted. However, this relation tells us that NR is particularly sensitive to sharp composition gradients where there is significant difference in contrast (i.e., different scattering lengths) between the two components. For shallow composition gradients it is much more difficult to obtain a unique depth profile as much of the information is located at wave vectors corresponding to total reflection. We analyze our NR data using two different approaches. The first is a model fitting method as described elsewhere [53]. A model profile is fitted to the data by adjusting parameters using a downhill simplex routine [54]. This method restricts the experimenter to a model form for the profile which may or may not be correct. In many cases, it is more desirable to use a technique capable of free form profiling such as simulated annealing [55] or maximum entropy (MaxEnt) [18,56]. In free form methods the film is split into a large number of small intervals and the volume fraction obtained at each point. Of course, with a large number of free variables a large number of possible solutions will fit the data equally well; to determine which to choose requires some regularization scheme. Such a scheme, with some fundamental information theoretic justification, is provided by the maximum entropy method, which is described in more detail below.

Maximum entropy analysis of NR data

Optimal fitting procedures usually require that the unnormalized χ^2 lie within a range $N\pm(2N)^{1/2}$, where N is the number of data points. If one applies a free form method to a set of data, with little or no constraint on the result, and if one allows a large number of points to make up this free form result, then one can easily obtain values of χ^2 close to zero. As well as this, one creates a large number of possible solutions to the data. In short, if one attempts to fit data, then one must beware of fitting statistical noise within those data. Maximum entropy has its own protection against a large number of solutions. We choose the most probable profile of the possible set by defining, and maximizing, an entropy, which is proportional to the logarithm of this probability. The simple MaxEnt method makes no assumptions about the degree of correlation between neighboring intervals, and this tends to introduce into the solution unphysical small wavelength volume fraction fluctuations (spikes). In the modified MaxEnt method we use, this is prevented by an "intrinsic correlation function" (ICF) [57] which imposes a degree of smoothness on the volume fraction profiles reflecting our *a priori* knowledge that such short wavelength fluctuations are improbable.

If the film is assumed to be laterally homogenous, then we may take the composition-depth profile $\phi(z)$ to be

$$\phi(z)=\sum_{j=1}^{j=M}\phi_j\exp\left[-\frac{(z-j\Delta z)^2}{2\sigma^2}\right], \tag{1}$$

where the summation is over all of the M elements, Δz, of the film. The exponential term is the ICF [57] represented as a Gaussian of width σ. We wish to infer $\phi(z)$ from the reflectivity data and so we wish to maximize the conditional probability distribution function $P(\phi(z)|R(k))$. This may be evaluated by using Bayes' theorem:

$$P(R(k)|\phi(z))\propto P(\phi(z)|R(k))P(\phi(z)) \tag{2}$$

since the left-hand side is easier to obtain. This left-hand side may be related to the residual squared misfit statistic, if we assume the N data are subjected to independent

Gaussian additive noise, by

$$P(R(k)|\phi(z)) \propto \exp\left[-\frac{\chi^2 N}{2}\right] . \quad (3)$$

In such a free form fitting procedure the number of data and the number of fitting parameters are comparable and so least squares fitting is undesirable. We take advantage of the volume fraction profile being positive at all values of z and relate the probability density distribution to an entropy [58,59]

$$P(\phi(z)) \propto \exp(\alpha S) , \quad (4)$$

where α is a constant and the entropy is given by

$$S = \sum_{j=1}^{j=M} \left[\phi_j - m_j - \phi_j \ln \frac{\phi_j}{m_j}\right] , \quad (5)$$

where m_j is a suitable measure for the fit, often referred to as a default model since, in the absence of data, $\phi_j = m_j$ is the optimal solution. m_j is generally taken to be flat since we are usually ignorant as to the precise form of the probability density distribution. We may, however, choose a different prior if we do have preexisting knowledge from, say, NRA data. The Lagrange multiplier α is chosen such that $\chi^2 \sim 1$. This relationship is rather *ad hoc* but can be handled in a more rigorous way [57] and provides the basis for a fully quantitative maximum entropy analysis [60]. An algorithm for the implementation of (4) and (5) with the likelihood function (2) is given by Skilling and Bryan [61].

It is possible to obtain an estimate of the reliability about a given point. If we let Φ be the average value of the volume fraction between two points z_1 and z_2, then

$$\Phi = \frac{1}{z_2 - z_1} \int_{z_1}^{z_2} \phi(z) dz = \Phi_0 \pm \sigma \quad (6)$$

and a plot of the error bar as a function of the size of the symmetric interval $\pm(z_2 - z_1)/2$ yields a star-shaped object representing the reliability of our solution about a given point $\pm(z_2 + z_1)/2$ [62]. There is little point in calculating errors on individual points because the errors would be unrealistically large since adjacent points are correlated.

There are limitations to the procedure. Consider how the MaxEnt method works: first the routine tries to reduce χ^2 while trying to keep the entropy as large as possible. When (the unnormalized) χ^2 is approximately equal to the number of data points, N, the routine maximizes the entropy of the composition-depth profile. This is analogous to the entropic term in the free energy of a polymer mixture but with the constraint $\chi^2 \sim N$. As long as this constraint is satisfied, the MaxEnt method will try to come as close as possible to a uniform film. With this in mind shallow composition gradients are inhibited, despite the possibility of being physically real. However, this is more a limitation of NR than the MaxEnt method of analyzing data. If one knows *a priori* the theoretical form for the profile, then one may fit to that, but any other method will return a profile with a large associated error (although it is likely that the user will not be able to compute this error). MaxEnt will return the most *likely* profile, given the stated constraints.

The Gaussian smoothing function used in this implementation of MaxEnt also has an adverse affect on the intrinsically good resolution of NR as it tends to smooth out surfaces; it is much harder to obtain an accurate surface volume fraction using this technique. This does not mean that a 10 Å wide interface will not be revealed by MaxEnt because, if the contrast is good but the smoothing function width is kept small, then sharp interfaces can be obtained. There is always the danger that unwanted ringing will appear elsewhere in the profile when this is done, and indeed this was a problem in the miscible blend discussed in Sec. IV.

A limitation of a more practical nature with this method of data analysis is that one must know all the associated parameters of the experiment, for example, the error in the angle of the neutron beam, θ, and the resolution $(\Delta\theta/\theta)$. These parameters cannot be fitted with this method, except at the expense of a large computational demand.

MaxEnt is an ideal method for analyzing NR data when there is no known theoretical behavior, or where alternative possibilities may exist. It is computationally demanding given that many fitting parameters are necessary (for example, many of the fits in this paper used 250 points to form the composition profile). Even so, this MaxEnt method is a powerful free form fitting routine because of the twofold protection provided against spurious composition fluctuations.

III. PHASE DIAGRAM

One of the most important parameters required in order to reach a quantitative understanding of our results is the Flory-Huggins interaction parameter. For our two blends we have used a value obtained by previous workers, and a similar one obtained from our own experiments.

For the blend with the PαMS MW of 50 000, we use the value obtained by Lin and Roe [41] using light scattering and, setting this in the usual dimensionless form [63] based on a toluene lattice (with lattice parameter 5.61 Å), we obtain

$$\chi(\phi, T) = \frac{53.4}{T}(0.0626 - 0.0018\phi - 5.6\times10^{-5}T) , \quad (7)$$

where T is the temperature in degrees Kelvin. We have used densities of 1.132 and 1.073 g cm^{-3} for d-PS and PαMS, respectively, for calculating the polymerization indices.

This value is found to be $\sim$10% too small for the blend with a PαMS MW of 97 600 and so we multiply the above value by a constant term (see Sec. V) and obtain

$$\chi(\phi, T) = \frac{59.2}{T}(0.0626 - 0.0018\phi - 5.6\times10^{-5}T) . \quad (8)$$

The phase diagrams for these blends are shown in Fig. 1.

Two methods were used to obtain the above interaction parameters. The usual way to obtain an interaction parameter with polymer films is to create a bilayer of the

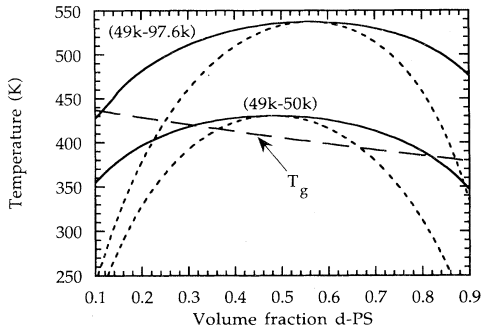

FIG. 1. The calculated phase diagrams for the two blends used in this study. The spinodals are the dashed lines and the binodals are the full lines. The glass transition temperature T_g for the blend is also included, calculated using the Fox equation [67] and values of T_g(*d*-PS)=100 °C and T_g(PαMS)=173 °C. T_g(PαMS) was measured for a MW equal to 97 600 by differential scanning calorimetry.

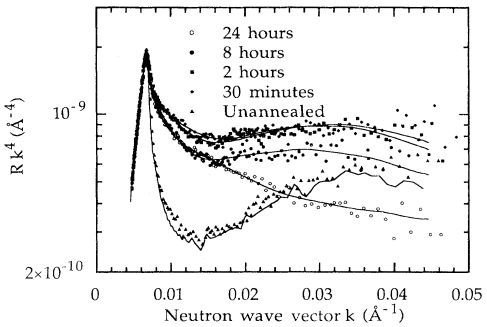

FIG. 2. Rk^4 profiles for five 4850 Å thick films of the 49*k*-50*k* blend with *d*-PS volume fraction 0.484. The samples were annealed for 0, 0.5, 2, 8, and 24 h at 180 °C. The values of χ^2 for these fits are 1.7, 2.2, 1.9, 2.5, and 1.2, respectively. The data for the unannealed sample were fitted using the MaxEnt routine with a Gaussian smoothing of width 75 Å and the data for the annealed samples were fitted using a simplex fitting routine.

two polymers, and to anneal them until they reach equilibrium, which will be at the coexisting volume fractions [9,10,64]. For the 49k-50k blend we use two layers that were nearly equal in composition ($\phi \approx 0.5$) and lowered the temperature, measuring the interdiffusion coefficient. As the critical point is approached, the interdiffusion coefficient tends to zero (thermodynamic slowing down [65]). This is a difficult method of measuring the interaction parameter, but as there was a positive interdiffusion coefficient down to temperatures of below 160 °C we accept the interaction parameter given by Lin and Roe [41] and presented in Eq. (7), which predicts an upper critical solution temperature of 157 °C. Such interdiffusion in miscible *d*-PS–PαMS bilayers is the subject of a separate study [66].

For the 49k-97.6k blend these experiments were more difficult; it was not possible to create a bilayer of the pure components without the *d*-PS dewetting from either the substrate or the PαMS layer, depending on the orientation of the film. If the layers contained *d*-PS volume fractions of 0.894 (top) and 0.038 (substrate) then dewetting did not occur but even after 18 days annealing at 180 °C, the film was not close to equilibrium. The alternative method used was to anneal films of varying bulk volume fractions and observe the equilibrium profile and, if the film was not at equilibrium, the depletion layer. (We assume incompressibility so the missing *d*-PS in the depletion layer is replaced by PαMS.) This method was used to obtain the adsorption isotherm and by assuming that the adsorbed amount diverges at the coexisting volume fraction, we were able to estimate this as $\phi_\alpha = 0.14 \pm 0.01$. From this we scaled Eq. (7) to obtain the interaction parameter for this blend [Eq. (8)].

IV. MISCIBLE SYSTEM

Surface segregation in the miscible (49*k*-50*k*) blend is not large compared to that observed in the other regions of the phase diagram discussed in this paper. Consequently, the resolution of NRA failed to reveal the amount of segregation, and so the experiments described in this section were performed using NR.

We have annealed four films with $\phi = 0.484$ for differing times at 180 °C and performed NR on these samples and on an unannealed one. The data and fits are shown in Fig. 2. The data were fitted to a model profile consisting of a complementary error function at the vacuum interface and an error function at the substrate, using a downhill simplex fitting routine [53] (see Fig. 3). The quality of the fits is generally good, indicating that this dual error function morphology describes the kinetics of the segregation. However, it was not possible to obtain an acceptable fit using the simplex routine for the unannealed sample. MaxEnt was used in this case, and shows PαMS segregating to the substrate in this sample. The MaxEnt routine was incapable of providing good fits to the samples annealed for 30 min and 2 h (the ICF had to be small in order to reveal the sharp interfaces in the profile and this resulted in unwanted composition fluctuations elsewhere). We do not believe that the *d*-PS is actually segregating to the substrate in the annealed samples; it is more likely that the technique is detecting a depletion layer to a PαMS-rich substrate layer (but MaxEnt results fail to detect this). The silicon substrate has a scattering length comparable to a *d*-PS volume fraction of 0.17, and so NR is not sensitive to whether or not there is a PαMS-rich segregating layer at the substrate. The effect of a silicon oxide layer is minimal, after a separate experiment performed on a bare substrate showed that an oxide layer did not contribute to the reflectivity profile in the k range used in these experiments.

Before discussing the kinetics of the segregation we compare the equilibrium segregation with standard mean field theory. Two samples, one annealed for 79 h at 176 °C and the other for 24 h at 180 °C, had similar composition profiles (see Fig. 3). The 79 h sample shows less segregation than the 24 h sample, and this may be attributed to the glass transition temperature of the PαMS slowing the kinetics down. We cannot say if the 24 h

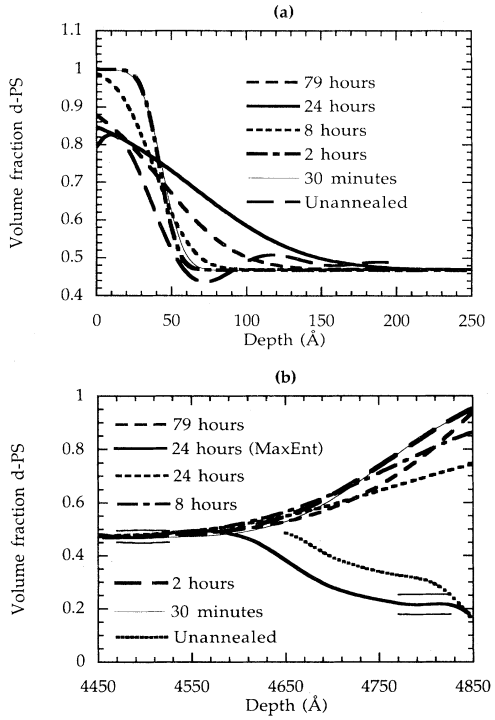

FIG. 3. Best fit profiles for the data shown in Fig. 2 and for a sample annealed at 176 °C for 79 h. The profiles for the annealed samples are error functions and the unannealed profile is a free form solution using the MaxEnt fitting routine. In both cases the 2 h and 30 min samples have very similar profiles. The profiles in (a) show segregation to the vacuum interface ($z=0$) and in (b) to the substrate interface ($z=4850$ Å). We believe that at the substrate these profiles are of depletion layers, and the substrate is enriched in a layer of PαMS not detected by the neutron reflection experiments (see text). In (b) we include a MaxEnt profile for the 24 h sample, with error stars.

sample is at equilibrium but we assume that it is because the quality of the NR fit indicates that there is no significant depletion layer present behind the segregated layer (a depletion layer implies that the sample has not reached equilibrium). Also, separate interdiffusion measurements [66] show that the interdiffusion coefficient at $\phi=0.5$ is $\sim 10^{-14}$ cm^2 s^{-1}, giving a diffusion length of over 500 Å for a time of 1 h. Of course, this length would be considerably smaller if a depletion layer was present due to the high T_g of PαMS.

We can use mean field theory to estimate the bare surface free energy. We use a surface energy f_s of the form given by Schmidt and Binder [22]:

$$f_s(\phi_1)=-\mu_1\phi_1-\frac{s\phi_1^2}{2}\ , \tag{9}$$

where μ_1, ϕ_1, and s are a surface chemical potential difference, surface volume fraction, and a surface interaction parameter, respectively. The bare surface energy difference $\Delta\gamma$ between the polymers is related to these terms by

$$\Delta\gamma=\frac{k_BT}{b^3}\left[\mu_1+\frac{s}{2}\right]\ , \tag{10}$$

where b is the lattice parameter and k_B is Boltzmann's constant. We relate the bulk and surface interaction parameters by $s=-b\chi$ [3,14,30], and, after substituting into the minimized free energy functional [35], we obtain

$$\frac{b^3\Delta\gamma}{k_BT}-b\chi\left[\phi_1-\frac{1}{2}\right]=\frac{a}{3}\left[\frac{G(\phi_1)-G(\phi_\alpha)-(\phi_1-\phi_\alpha)\Delta\mu_\alpha}{\phi_1(1-\phi_1)}\right]^{1/2} \tag{11}$$

in the same manner as used for d-PS–h-PS films [2]. The symbols have their usual meanings: a is the statistical segment length (we use 6.7 Å for this blend), $G(\phi)$ is the Gibbs free energy of mixing, $\Delta\mu$ is the exchange chemical potential, and the subscript α refers to evaluation at the lower coexistence value. The solution to this equation yields a bare surface energy difference of 0.27 mJ m^{-2}, and this can be compared with 0.08 mJ m^{-2} for the isotopic polystyrene blend [2,3], and 0.14 mJ m^{-2} for a blend of d-PS and poly(styrene-co-4-bromostyrene) random copolymer [17]. We estimate an error of about 0.05 mJ m^{-2} by comparing with the NR data for the film annealed at 176 °C for 79 h.

The mean field composition profile $z(\phi)$ is given by [2,3,35]

$$z=\frac{a}{6}\int_{\phi_\infty}^{\phi_1}\frac{d\phi}{\{\phi(1-\phi)[G(\phi)-G(\phi_\infty)-(\phi-\phi_\infty)\Delta\mu_\infty]\}^{1/2}}\ . \tag{12}$$

This profile is calculated and shown, with that obtained from the fit to the 24 h data, in Fig. 4. The experimental profile shows slightly more segregation than the mean field prediction, which has a larger decay length. A qualitatively similar discrepancy has been observed before [5], but the reason for this difference is not known. One possibility is that the discrepancy is caused by the segregation of chain ends to the interface [7]. Such conformational changes near the surface are not included in the

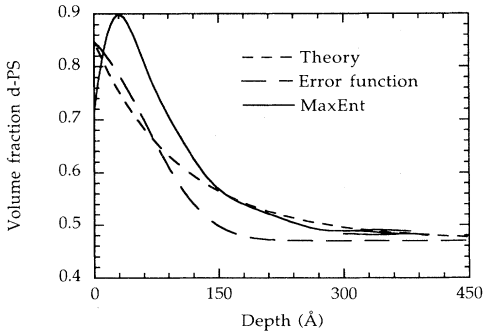

FIG. 4. Depth profiles from the vacuum surface into the bulk of a film containing 0.484 d-PS annealed for a day at 180 °C (obtained by the simplex and MaxEnt methods) and the theoretical equilibrium calculation. An error star is shown for the MaxEnt method.

simple mean field theory so it is not surprising that the mean field prediction of Schmidt and Binder [22] fails. A detailed study of films of an isotopic polyethylenepropylene blend [16] has shown that correlations between chains, as well as chain conformations, may also affect the surface profile. Other workers have modified the surface energy with some success [6,32], and self-consistent field calculations have predicted the shape of the profiles for *d*-PS–*h*-PS films [19]. Long range forces have been postulated as possible candidates to explain this discrepancy [33] but Jones [26] has shown by model calculations that they have a negligible effect on segregation profiles in the one phase region.

We have included in Fig. 3(b) the substrate profile determined by MaxEnt for the 24 h sample but for clarity we show the corresponding vacuum interface profile in Fig. 4. The value of χ^2 for the MaxEnt fit was 1.4, close to the value for the simplex fit. The MaxEnt vacuum interface profile, on the face of it, appears to show much more segregation than that obtained from the model fitting routine. If one allows for the offset caused by surface roughness effects in the MaxEnt analysis then the profiles become more alike. The shape of the near surface region is not revealed by the MaxEnt analysis because of the effect of the ICF of width 75 Å. Since adjacent points in the profile are correlated, the error stars are small, and these are shown in the figures. Error stars associated with the substrate profile are greater than at the vacuum interface. In regions where there is a rapid variation in volume fraction error stars are unreliable since they are taken over the average volume fraction in the region of interest; if this volume fraction is rapidly varying the average volume fraction has a large associated standard deviation and the error star cannot be considered accurate.

Turning now to the kinetics of surface segregation, we see rather puzzling behavior. The sample does not start out homogenous, presumably because some segregation takes place during the spin casting process. On annealing, the surface volume fraction rises almost to unity, but the segregation is confined to a narrow layer within a radius of gyration ($\sim$56 Å) of the surface. Only after much longer annealing times does the near surface depth profile assume the expected exponential-like decay.

A possible cause of this behavior lies in the strong composition dependence of the interdiffusion coefficient, which arises because the annealing temperature is close to the glass transition temperature of pure PαMS [48,65]. Initially a local rearrangement of chains near the surface happens relatively quickly as whole chain motions are not involved. This leaves a region just below the surface with a lower volume fraction of *d*-PS, where the local chain mobility is much lower than that for the homogenous bulk of the sample. We calculate that for a *d*-PS volume fraction of $\sim$0.2, the diffusion length for an annealing time of 2 h at 180 °C may be as small as 160 Å. The initial local motion occurs on a timescale not greater than the reptation time for the bulk composition [66,68], which is of the order of seconds [69], and it may be influenced by the attraction of chain ends to the surface [77].

V. WETTING LAYER GROWTH FOR OFF-CRITICAL QUENCHES

The most difficult part of the phase diagram to understand from a theoretical point of view is the metastable region. There has been little experimental study of polymer blend films quenched between the spinodal and binodal but there has been some theoretical work on this subject [20,22–25,27,31,34]. In the metastable region one phase may be preferentially attracted to the wall. If that phase is rich in the minority component of the film, and if it completely wets the wall it will, at equilibrium, be infinitely thick in a semi-infinite system in the absence of gravitational effects [35]. In this section we are concerned with the situation in which a *d*-PS phase completely wets the vacuum interface. We consider the growth of the subsequent wetting layer for three metastable quenches and a quench just inside the spinodal.

Here we use the partially miscible blend of *d*-PS and PαMS with respective molecular weights of 49 000 and 97 600. We created a series of films with *d*-PS volume fractions of 0.199, 0.230, 0.273, and 0.333 which were annealed at 180 °C for a variety of times (up to a week). The films containing *d*-PS volume fractions of 0.199 and 0.273 were studied by NRA and the other two by NR. The spinodal is estimated to be at a *d*-PS volume fraction of 0.28 and NRA on a $\phi_\infty = 0.333$ film indicated that there was, at least after 24 h, no evident surface directed spinodal decomposition profile (for a full discussion of this phenomenon, see the review by Krausch [71]). The NR data and MaxEnt fits are shown in Figs. 5 and 6 and the *d*-PS depth profiles in Figs. 7 and 8. For the MaxEnt fitting we found that there was no need to include segregation to the substrate in the fitting procedure as this had little effect on the profile. Typical NRA data and fits are included in Fig. 9. The values of χ^2 for the NR fits range between 1.4 and 3.8, so they are clearly satisfactory. The fits to the NRA data are the convolution of the sum of two error functions (one, a complementary error function, describes the growing face of the wetting layer and the other, the interface between the depletion layer and the bulk) with a Gaussian resolution function of 175 Å width.

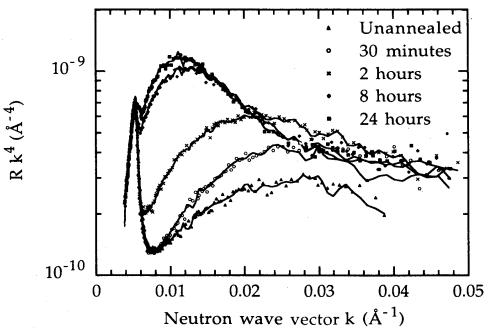

FIG. 5. NR data and best MaxEnt fits for films containing a *d*-PS volume fraction of 0.230 for the 49k-97.6k blend after annealing at 180 °C for 0, 0.5, 2, 8, and 24 h. The values of χ^2 for the fits are 2.0, 2.4, 1.4, 1.5, and 1.4, respectively.

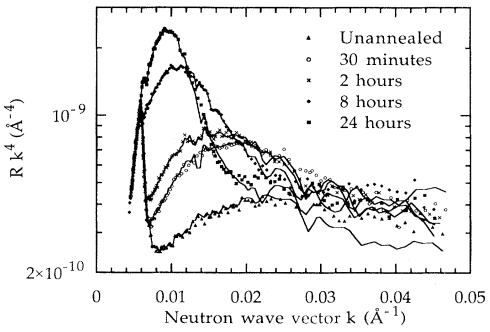

FIG. 6. NR data and best MaxEnt fits for films of the 49k-97.6k blend containing a *d*-PS volume fraction of 0.333 after annealing at 180 °C for 0, 0.5, 2, 8, and 24 h. The values of χ^2 for the fits are 2.4, 3.8, 1.7, 1.9, and 3.3, respectively.

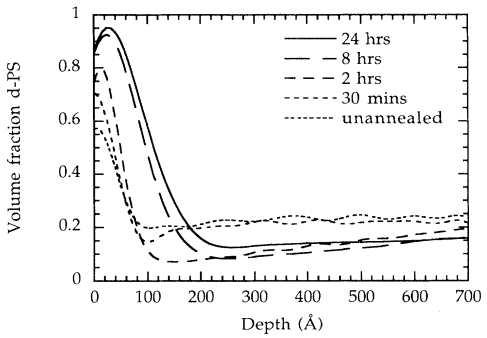

FIG. 7. Volume fraction profiles for the fits included in Fig. 5. We show the first 700 Å of the profiles. The films have a total thickness of 5000 Å but we have only fitted to the first 700 Å (unannealed and 30 min), 1200 Å (2 h), and 2000 Å (8 and 24 h). The following Gaussian smoothing widths have been employed: 100 Å (unannealed and 30 min), 75 Å (2 h), and 125 Å (8 and 24 h).

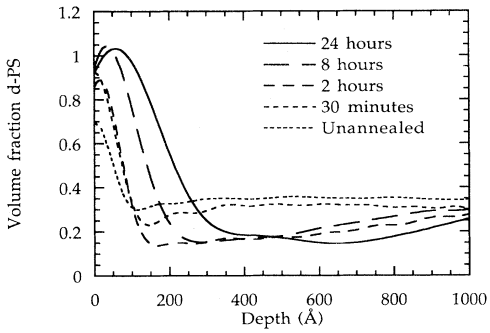

FIG. 8. Volume fraction profiles for the fits included in Fig. 6. We show the first 1000 Å of the profiles. The films have a total thickness of 4700 Å and we have fitted the first 4700 Å (the entire film thickness for the unannealed film), 1000 Å (30 min), 1500 Å (2 h), 2000 Å (8 h), and 3000 Å (24 h) of the profile to the data. The following Gaussian smoothing widths have been employed: 125 Å (unannealed and 2 h), 150 Å (30 min and 8 h), and 250 Å (24 h).

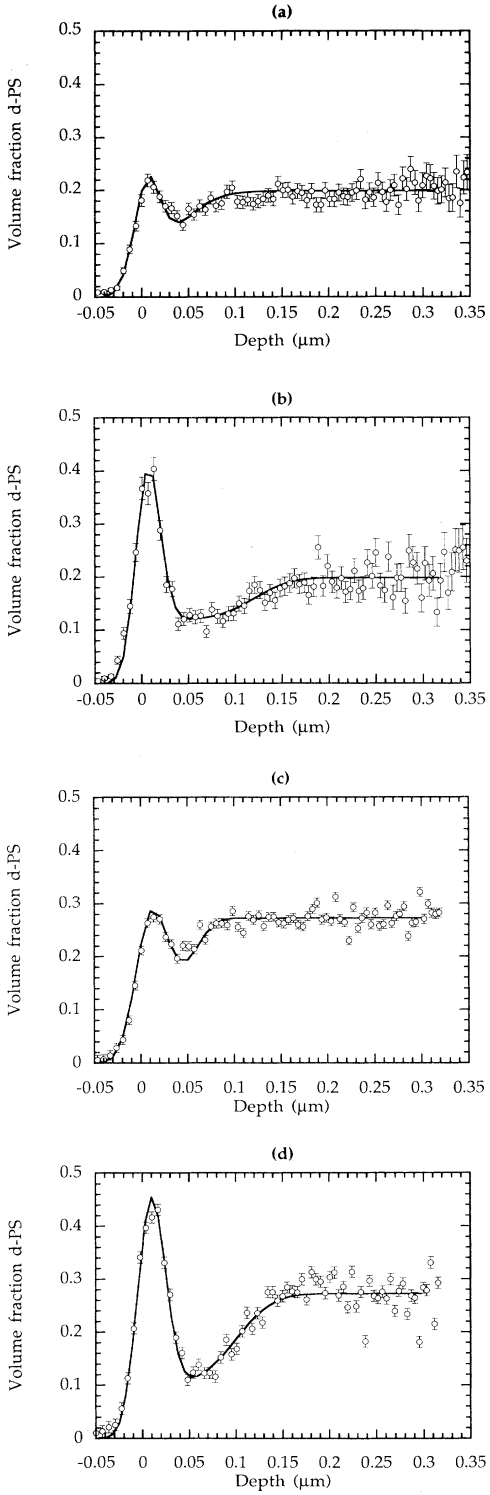

FIG. 9. Some of the NRA data and fits for films annealed at 180 °C, quenched inside the metastable region of the phase diagram. (a) shows a film with $\phi_\infty = 0.199$ after annealing for 2 h. (b) shows a film with $\phi_\infty = 0.199$ after annealing for 24 h. (c) shows a film with $\phi_\infty = 0.273$ after annealing for 30 min. (d) shows a film with $\phi_\infty = 0.273$ after annealing for 48 h. The fits were obtained by convolving a series of error functions with the Gaussian resolution function of the NRA experiment.

A. Adsorption isotherm

In order to analyze our data we need to know the surface excess as a function of volume fraction as one approaches the coexistence curve from the one phase region. We prepared films of different bulk volume fractions of d-PS and annealed them for between 18 and 19 d at 180 °C. The surface excess was measured for these samples. Some of the samples had not reached equilibrium but no attempt was made to anneal these for longer since this increases the risk of oxidation or degradation in the vacuum oven. Fortunately, in the samples that had not reached equilibrium, the experimental resolution did not prevent a measurement of the depth of the depletion layer, and so we were able to calculate the surface excess for the measured volume fraction in the depletion layer (we assume the surface layer to be in local equilibrium with the depletion layer). We show in Fig. 10 NRA data for two samples: one that reached equilibrium, and one that did not. The adsorption isotherm is included in Fig. 11 along with a fit. From the adsorption isotherm we were able to measure the volume fraction of d-PS on the binodal, ϕ_α, and so estimate the interaction parameter. We estimate $\phi_\alpha = 0.14 \pm 0.01$. From Cahn's theory of wetting [35] we expect the adsorbed amount to diverge as $z^* = -A \ln[(\phi_\infty - \phi_\alpha)/\phi_\infty]$. We obtain a much better fit if we include a term linear in ϕ to give the following adsorption isotherm:

$$z^* = 161\phi - 35.6 \ln\left[\frac{0.14-\phi}{0.14}\right] . \quad (13)$$

The form of the fit was chosen so as to give an acceptable fit while still showing a monotonic increase in z^* with ϕ, although we note that the approach to coexistence from the one phase region can be more complicated than this model suggests [8,32]. We should note that in polymer blend films the coefficient of the squared gradient term in the Cahn-Hilliard free energy [37] is given by the random phase approximation and is composition dependent [63,72].

It is interesting to consider that the surface excess measured for the smallest bulk value ($\phi_\infty = 0.038$) of 21.3 Å for a deletion layer volume fraction of 0.29 ± 0.03 corresponds to a surface volume fraction of 1. The surface energy cannot be calculated from this as the error involved would be too large. Also, the Schmidt and Binder surface energy is no longer valid as surface entropy terms must be included in the surface energy [6,32]. We conclude that the surface energy is greater for this blend than for the miscible blend, in keeping with the general MW dependence of polymer surface energy, and in qualitative agreement with other experimental results for polymer blend films [1,11,12,73]. Calculations using (7) for the interaction parameter for this blend have shown that we are on the wetting side of a wetting transition [48]; the complete wetting of the surface for the lowest d-PS volume fraction further underlines this point.

B. Model

The approximation that we make is to assume that the diffusion layer is in local equilibrium with the wetting layer. This assumption, first made by Lipowsky and Huse [74], is valid if the diffusion length of the blend is greater than the size of the wetting layer. In this approximation one solves the diffusion equation subject to a partially reflecting boundary condition which ensures the lo-

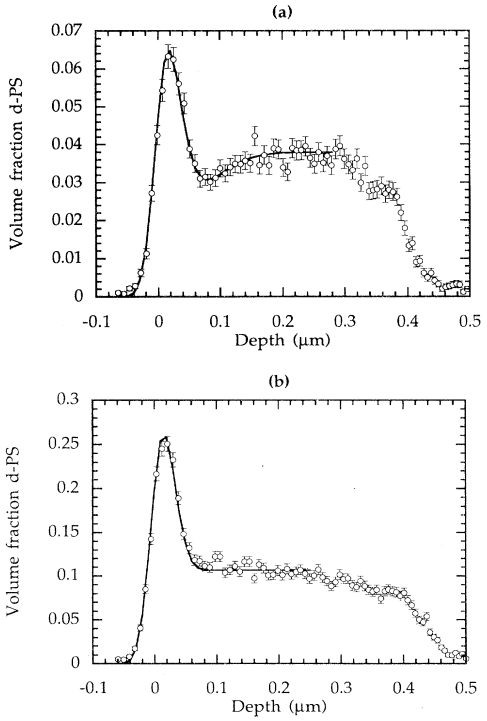

FIG. 10. NRA data for a sample with (a) $\phi_\infty = 0.038$ and (b) $\phi_\infty = 0.107$ after annealing at 180 °C for ~18 d. In the first case the surface layer had not equilibrated, while in the second, it had. The shape of the profile at the back of the film provides convincing evidence that the PαMS segregates preferentially to the substrate.

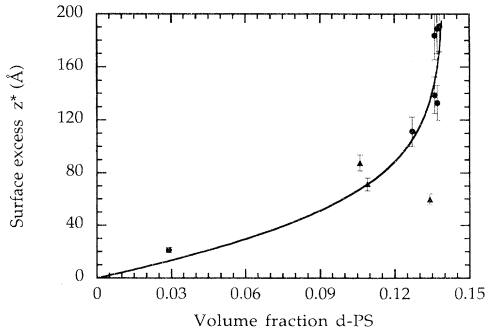

FIG. 11. Adsorption isotherm data and fit. The full triangles are equilibrium profiles, while the full circles were obtained after assuming the surface enriched layer was in local equilibrium with the depletion layer. All data were obtained after annealing at 180 °C for periods of ~18 d. The error bars are 7% of z^* (equilibrium) and 10% (where the depletion layer volume fraction is measured).

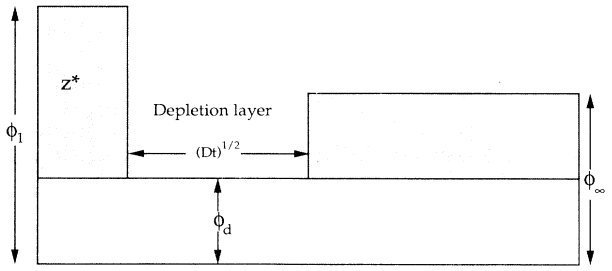

FIG. 12. Schematic diagram illustrating the model of Jones and Kramer [4].

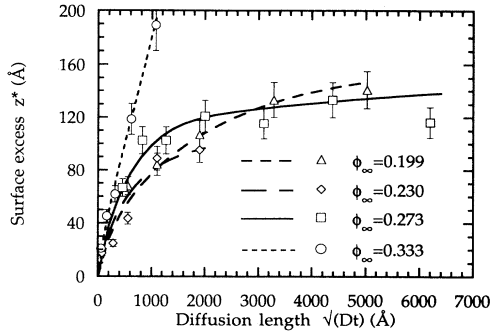

FIG. 13. z^* plotted against diffusion length for the growth of wetting layers. The data are fitted to a numerical solution of Eq. (16).

cal equilibrium condition is met [4]. An even simpler treatment eliminates the need to solve the diffusion equation exactly (which in most cases requires numerical solutions) by approximating the depletion zone behind the surface peak as a region of uniform concentration, ϕ_d, extending to a depth of the diffusion length $(Dt)^{1/2}$ (see Fig. 12). It turns out that the results of such a simplified model are in surprisingly close quantitative agreement with full numerical solutions of the diffusion equation with appropriate boundary conditions [13]. This model has given excellent agreement in describing the growth of surface segregated layers in *d*-PS–*h*-PS films [4,13].

The growth of wetting layers in binary films where the composition is in the metastable part of the phase diagram is expected to be a three stage process [13]. The initial and final stages are diffusion limited and grow as $t^{1/2}$ [74]. Separating these two stages is a region of logarithmic growth. The logarithmic growth is caused by the depletion layer volume fraction becoming close to the binodal value, so that it is slightly undersaturated, a situation that has been shown to cause the wetting layer thickness to logarithmically diverge with the difference in volume fraction from the binodal [35]. We obtain for the surface excess [4]

$$z^*(\phi_d(t))=[\phi_\infty-\phi_d(t)](Dt)^{1/2}\ , \tag{14}$$

where D is the diffusion coefficient and ϕ_∞ and ϕ_d the bulk and depletion layer volume fractions, respectively. In our analysis we substitute for ϕ_d in Eq. (14) the adsorption isotherm obtained above [Eq. (13)]; the local equilibrium assumption amounts to the equation of $z^*(\phi_d(t))$ with $z^*(\phi)$.

C. Results

The results of z^* against $t^{1/2}$ are plotted in Fig. 13. NR measurements revealed small surface excesses (17.4 and 20.9 Å) in the unannealed $\phi_\infty=0.230$ and 0.333 films, respectively, presumably due to segregation occurring during the spin casting process. To account for this, the time was adjusted by adding an offset t_0, where $z^*(t=0)=\phi_\infty(Dt_0)^{1/2}$. The NRA data were similarly adjusted using the NR data, since the resolution of the NRA experiment was not good enough to obtain these small values of z^*.

The simple model described above is not a good enough description of our films; we tried to obtain good fits to the data using this model by altering the diffusion coefficient, which, since the adsorption isotherm is known, is the only variable. There are at least two possible reasons why our simple model might fail. First, the interdiffusion coefficient in this system has a concentration dependence, due to the differing glass transition temperatures of the two components. However, numerical solutions of the diffusion equation with a realistic (exponential) composition dependence did not provide better fits to our data. The second possibility is that phase separation in the bulk of the film competes with the segregation. Incomplete phase separation could occur during the casting process or during the time it takes the sample to achieve its annealing temperature as well as during annealing. The resulting phase separated domains will be rich in *d*-PS and will lower the bulk (matrix) volume fraction, effectively slowing down the wetting layer growth. We need to introduce a term to describe this loss of *d*-PS from the bulk. We choose an empirical form which meets the requirements that at time $t=0$ the matrix volume fraction $\phi_m=\phi_\infty$, and for long times it tends asymptotically to the coexisting volume fraction; the form we choose is

$$\phi_m=\phi_\infty-(\phi_\infty-\phi_\alpha)\mathrm{erf}(at^\delta) \tag{15}$$

where ϕ_α is the binodal volume fraction and a is a variable. We then return to the simple model of Jones and Kramer [4] and equate the material flux at the surface as dz^*/dt (from conservation of material). From Fick's first law this is equal to the product of the diffusion coefficient and the concentration gradient. We write this as [75]

$$\frac{dz^*}{dt}=\left[\frac{D}{4t}\right]^{1/2}[\phi_m-\phi_d(z^*)] \tag{16}$$

and substitute for ϕ_m using Eq. (15). This equation is then numerically solved for z^*. We find that $\delta=\frac{1}{2}$ gives better fits than $\delta=\frac{1}{3}$. We include, in Fig. 13, the best results that we obtained by adjusting D and a, and these values are tabulated in Table I. The fits show good agreement with the data but we see that there was no one value of D or a that we could settle on since they vary

TABLE I. Values of D and a obtained for the four different values of ϕ_∞, obtained after fitting to the modified Eq. (16) [using Eq. (15)].

ϕ_∞	D (10^{-15} cm^2 s^{-1})	a (10^{-3} s$^{-1/2}$)	Method
0.199	4.2	1.7	NRA
0.230	4.2	5.0	NR
0.273	11.1	7.5	NRA
0.333	1.3	0.5	NR

over factors of 8.5 and 15, respectively. Nevertheless, the form for the loss of d-PS is empirical and we can be confident that we are qualitatively explaining the film behavior.

D. Discussion

In this discussion we consider limitations of our analysis. First we consider the composition dependence of the diffusion coefficient. Further limitations of the model itself are then discussed before we point out a weakness in our analysis of NR data. Finally, we refer to the growth of wetting layers close to the spinodal. The need for further experiments is emphasized, and a suggestion is made as to what could be performed.

The diffusion coefficient is composition dependent; thermodynamic slowing down will reduce D near the binodal [65] and the high T_g of PαMS reduces D for small ϕ. Any full numerical solution to the diffusion equation, or indeed to our simple model, needs to account for this. Since D varies over a factor of 8.5 in our simulations we see that these effects must exist.

If there are d-PS-rich domains in the bulk of the film, then we cannot assume that domains are not present in the depletion layer, particularly since the depletion layer is moving in the direction of the bulk. If these domains exist they will contribute a growth exponent that has not been accounted for. The laterally averaged depletion layer volume fraction, as measured, is then incorrect in our analysis and the wetting layer must be in local equilibrium with the depletion layer matrix. Domains in the depletion layer are expected to be more significant at later times after the depletion layer has penetrated deeper into the bulk of the film. Domains present in the film close to (or inside) the depletion layer are likely to be anisotropic. The coalescence of anisotropic domains close to a wall has been shown to have a significant effect on wetting layer growth [76].

A further problem is due to the insensitivity of NR to shallow gradients. There is a tendency for the MaxEnt analysis to underestimate the surface excess because of overestimating the depletion layer volume fraction. To some extent this is compensated by a surface offset caused by the Gaussian smoothing.

We show in Fig. 14 the loss of d-PS to bulk domains [Eq. (15)] as a function of diffusion length using the parameters tabulated in Table I. The loss for the $\phi_\infty=0.333$ data follows a $t^{1/2}$ growth law but there is neither enough time nor enough data to fully ascertain

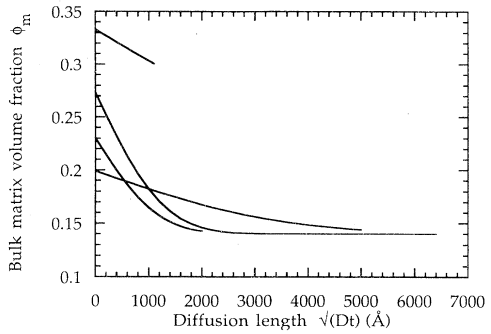

FIG. 14. The loss of d-PS from the bulk matrix to phase separated bulk domains [using the parameters tabulated in Table I and Eq. (15)] for the four values of ϕ_∞ is shown plotted against diffusion length.

the power law for the loss of material from the matrix. The $\phi_\infty=0.273$ data show a much more dramatic loss, reaching the binodal volume fraction within the timescale of the experiments. The $\phi_\infty=0.273$ and the $\phi_\infty=0.333$ data lie on either side of, but close to, the estimated spinodal, confirming that the region close to the spinodal is very interesting and would benefit from further study.

Some of the NRA data showed a "tail" following the depletion layer (see Fig. 15). This was not present in all of the samples and the cause of it is not clear. It is hard to overemphasize that the boundary between the metastable and unstable regions of the phase diagram is, at best, fuzzy. There are possible explanations for this behavior and we discuss two. These suggestions can only be speculative since the behavior of films in this region of the phase diagram is not well understood. The first is that the profile could be due to surface directed spinodal decomposition. A problem with this possibility is that there is no d-PS-rich depletion layer towards the substrate whereas in a separate study of these polymers in a deeper quench [77] such a layer did exist.

It is possible that domains in the bulk, but adjacent to the depletion layer, may compete with the wetting layer in attracting d-PS from the depletion layer. This d-PS

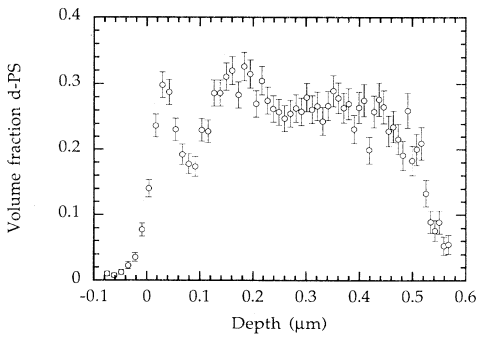

FIG. 15. NRA data for a film with $\phi_\infty=0.273$, annealed for 48 h at 180 °C. The data shown in Fig. 9(d) were obtained from NRA experiments on the same film but the $^3He^+$ beam was incident at an angle of 15°, whereas in this case the beam was incident at an angle of 30°.

will condense on the domains in the bulk, enhancing the amount of d-PS relative to the bulk. Such a condensation behavior is similar to a situation where such tails have been predicted for late time coarsening in which the majority phase wets the interface [34]. In this case, the tails come about through droplet condensation after the depletion layer (initially rich in the majority phase) crosses the spinodal. (We do note that we do not see such a behavior at the substrate possibly because the glassy PαMS-rich substrate phase is preventing any test of these predictions.)

We have mentioned several factors that could be taken into account in a complete and rigorous analysis of the data: composition dependent diffusion coefficient, domains in the depletion layer, and limitations in the MaxEnt profiles, but it is unlikely that these alter our conclusions.

Since these experiments are restricted to a narrow temperature window (the glass transition and the polymer degradation temperature essentially restrict us to experiments between 180 and 190 °C) it was not possible to prepare samples at elevated temperatures in the one phase region before quenching into the metastable region. If this was possible then one may begin to understand to what extent nucleation and growth has affected the morphology. Clearly, for a fuller understanding of metastable films, more studies of this behavior are necessary.

VI. SUMMARY AND CONCLUSIONS

We have performed a study of surface interactions on d-PS–PαMS in both the miscible and metastable parts of the phase diagram. For a miscible blend we have obtained a surface energy difference and the form for the equilibrium surface profile which compare well with experiments on d-PS–h-PS films. A mean field analysis provides an acceptable explanation of this profile. We also considered the kinetics of the growth of the surface layer. At early times local chain motion is important as a d-PS monolayer exists at the surface, and these conformational changes dominate the kinetics in a way not predicted by mean field theory.

Wetting layer growth in an off-critical quench in the metastable region of the phase diagram was studied. We assumed that the growing wetting layer is in local equilibrium with its depletion layer and found that the simple model of Jones and Kramer [4] provides a good explanation of the behavior if bulk nucleation and growth is considered. This slows down the growth of the wetting layer by depleting the bulk matrix of d-PS. We obtain diffusion coefficients for four sets of experiments between 1.3×10^{-15} and 1.1×10^{-14} cm^2 s^{-1}.

Many important questions remain unanswered. For example, in the miscible blend, the early stage kinetics are different from those for d-PS–h-PS films [13]. Why is this? Is it related to the inhomogenous unannealed sample, the nature of the surface energy, or the proximity to a glass transition? For films quenched between the coexistence curve and the spinodal we would like to see how the kinetics of the growth of wetting layers behave when quenched from the one phase region to limit nucleation sites. When do fluctuations become significant, and what is their effect? How do these films behave near the critical point, or how do they behave when crossing the spinodal? We hope that this work inspires experimentalists and theorists alike to attack some of the many problems remaining in this interesting and challenging field.

ACKNOWLEDGMENTS

We thank the SERC, ICI Plc, and the Colloid Initiative, sponsored by the Department of Trade and Industry, Unilever Plc, Schlumberger Cambridge Research, and ICI Plc for funding. M.G. is grateful for financial support from the SERC and ICI Plc. We thank Dr. Simon Butler of the Melville Laboratory for performing GPC and Chas Setterfield of the Department of Materials Science and Metallurgy for performing TGA on the PαMS (both are at the University of Cambridge). Dr. Chris Clarke, Dr. Abigail Ball, Dr. Steve King, Dr. John Webster, and Dr. David Bucknall all helped in obtaining NR data. We thank Maximum Entropy Data Consultants Ltd. for the use of the MemSys 4 maximum entropy computer program. Finally, M.G. would like to acknowledge Dr. Randal Richards and Dr. Athene Donald for their comments on this work.

[1] Q. S. Bhatia, D. H. Pan, and J. T. Koberstein, Macromolecules **21**, 2166 (1988).

[2] R. A. L. Jones, E. J. Kramer, M. H. Rafailovich, J. Sokolov, and S. A. Schwarz, Phys. Rev. Lett. **62**, 280 (1989).

[3] R. A. L. Jones, E. J. Kramer, M. H. Rafailovich, J. Sokolov, and S. A. Schwarz, in *Interfaces between Polymers, Metals and Ceramics,* edited by B. M. DeKovem, A. J. Gellman, and R. Rosenberg, MRS Symposium No. 153 (Materials Research Society, Bellingham, WA, 1989), p. 133.

[4] R. A. L. Jones and E. J. Kramer, Philos. Mag. B **62**, 129 (1990).

[5] R. A. L. Jones, L. J. Norton, E. J. Kramer, R. J. Composto, R. S. Stein, T. P. Russell, A. Mansour, A. Karim, G. P. Felcher, M. H. Rafailovich, J. Sokolov, X. Zhao, and S. A. Schwarz, Europhys. Lett. **12**, 41 (1990).

[6] X. Zhao, W. Zhao, J. Sokolov, M. H. Rafailovich, S. A. Schwarz, B. J. Wilkens, R. A. L. Jones, and E. J. Kramer, Macromolecules **24**, 5991 (1991).

[7] W. Zhao, X. Zhao, M. H. Rafailovich, J. Sokolov, R. J. Composto, S. D. Smith, M. Satkowski, T. P. Russell, W. D. Dozier, and T. Mansfield, Macromolecules **26**, 561 (1993).

[8] F. Bruder and R. Brenn, Europhys. Lett. **22**, 707 (1993).

[9] A. Budkowski, U. Steiner, and J. Klein, J. Chem. Phys. **97**, 5229 (1992).

[10] U. Steiner, J. Klein, E. Eiser, A. Budkowski, and L. J. Fetters, Science **258**, 1126 (1992).

[11] P. P. Hong, F. J. Boerio, and S. D. Smith, Macromolecules **27**, 596 (1994).

[12] A. Hariharan, S. K. Kumar, and T. P. Russell, J. Chem. Phys. **98**, 4163 (1993).

[13] M. Geoghegan, T. Nicolai, J. Penfold, and R. A. L. Jones (unpublished).

[14] A. Hariharan and S. K. Kumar, Macromolecules **24**, 4909 (1991).
[15] U. Steiner, J. Klein, and L. J. Fetters, Phys. Rev. Lett. **72**, 1498 (1994).
[16] L. J. Norton, E. J. Kramer, F. S. Bates, M. D. Gehlsen, R. A. L. Jones, A. Karim, G. P. Felcher, and R. Kleb, Macromolecules **28**, 8621 (1995).
[17] B. Guckenbiehl, M. Stamm, and T. Springer, Coll. Surf. A **86**, 311 (1994).
[18] I. Hopkinson, F. T. Kiff, R. W. Richards, S. Affrossman, M. Hartshorne, R. A. Pethrick, H. Munro, and J. R. P. Webster, Macromolecules **28**, 627 (1995).
[19] J. Genzer, A. Faldi, and R. J. Composto, Phys. Rev. E **50**, 2373 (1994).
[20] H. Nakanishi and P. Pincus, J. Chem. Phys. **79**, 997 (1983).
[21] H. Nakanishi and M. E. Fisher, J. Chem. Phys. **78**, 3279 (1983).
[22] I. Schmidt and K. Binder, J. Phys. (Paris) **46**, 1631 (1985).
[23] K. K. Mon, K. Binder, and D. P. Landau, Phys. Rev. B **35**, 3683 (1987).
[24] J.-S. Wang and K. Binder, J. Chem. Phys. **94**, 8537 (1991).
[25] I. Carmesin and J. Noolandi, Macromolecules **22**, 1689 (1989).
[26] R. A. L. Jones, Phys. Rev. E **47**, 1437 (1993).
[27] R. A. L. Jones, Polymer **35**, 2160 (1994).
[28] P. Cifra, F. E. Karasz, and W. J. MacKnight, Macromolecules **25**, 4895 (1992).
[29] P. Cifra, F. Bruder, and R. Brenn, J. Chem. Phys. **99**, 4121 (1993).
[30] R. A. Jerry and E. B. Nauman, Phys. Lett. A **167**, 198 (1992).
[31] S. Puri and K. Binder, Z. Phys. B **86**, 263 (1992).
[32] S. M. Cohen and M. Muthukumar, J. Chem. Phys. **90**, 5749 (1989).
[33] Z. Y. Chen, J. Noolandi, and D. Izzo, Phys. Rev. Lett. **66**, 727 (1991).
[34] G. Brown, A. Chakrabarti, and J. F. Marko, Phys. Rev. E **50**, 1674 (1994).
[35] J. W. Cahn, J. Chem. Phys. **66**, 3667 (1977).
[36] J. D. van der Waals, Z. Phys. Chem. **13**, 657 (1894); an English translation is given by J. S. Rowlinson, J. Stat. Phys. **20**, 197 (1979).
[37] J. W. Cahn and J. E. Hilliard, J. Chem. Phys. **28**, 258 (1958).
[38] L. D. Landau and E. M. Lifshitz, *Statistical Physics,* 3rd ed. (Pergamon, Oxford, 1980), Pt. 1.
[39] S. Saeki, J. M. G. Cowie, and I. J. McEwan, Polymer **24**, 60 (1983).
[40] J.-M. Widmaier and G. Mignard, Eur. Polym. J. **23**, 989 (1987).
[41] J.-L. Lin and R.-J. Roe, Macromolecules **20**, 2168 (1987).
[42] J.-L. Lin and R.-J. Roe, Polymer **29**, 1227 (1988).
[43] A. Rameau, Y. Gallot, P. Marie, and B. Farnoux, Polymer **30**, 386 (1989).
[44] H. Yang, S. Ricci, and M. Collins, Macromolecules **24**, 5218 (1991).
[45] J. M. G. Cowie, M. D. Fernandez, M. J. Fernandez, and I. J. McEwan, Polymer **33**, 2744 (1992).
[46] PαMS is known to degrade upon pyrolysis yielding only monomer [47] and in order to check its temperature stability we carried out the following tests. Gel permeation chromatography (GPC) was performed on some PαMS (MW equal to 97 600) before and after annealing at 180 °C for a day. The result indicated negligible molecular weight degradation of the PαMS on annealing [48]. A thermal gravimetric analysis (TGA) experiment also indicated that the polymer was stable, with respect to decomposition to monomer, under annealing, since negligible mass change was observed after 16.5 h at 185 °C.
[47] S. L. Madorsky, *Thermal Degradation of Organic Polymers* (Wiley-Interscience, New York, 1964).
[48] M. Geoghegan, Ph.D. thesis, University of Cambridge, Cambridge, 1994.
[49] J. Penfold and R. K. Thomas, J. Phys. Condens. Matter **2**, 1369 (1990).
[50] T. P. Russell, Mater. Sci. Rep. **5**, 171 (1990).
[51] R. S. Payne, A. S. Clough, P. Murphy, and P. J. Mills, Nucl. Instrum. Methods Phys. Res. Sect. B **42**, 130 (1989).
[52] J. Penfold, R. C. Ward, and W. G. Williams, J. Phys. E **20**, 1411 (1987).
[53] R. A. L. Jones, L. J. Norton, K. R. Shull, E. J. Kramer, G. P. Felcher, A. Karim, and L. J. Fetters, Macromolecules **25**, 2359 (1992).
[54] W. H. Press, S. A. Teukolsky, W. T. Vetterling, and B. P. Flannery, *Numerical Recipes in FORTRAN: The Art of Scientific Computing,* 2nd ed. (Cambridge University, Cambridge, 1992).
[55] K. Kunz, J. Reiter, A. Götzelmann, and M. Stamm, Macromolecules **26**, 4316 (1993).
[56] D. S. Sivia, W. A. Hamilton, and G. S. Smith, Physica B **173**, 121 (1991).
[57] S. F. Gull, in *Maximum Entropy and Bayesian Methods: Cambridge 1988,* edited by J. Skilling (Kluwer, Amsterdam, 1989), p. 53.
[58] J. Skilling, in *Maximum Entropy and Bayesian Methods: Cambridge 1988* (Ref. [57]), p. 45.
[59] J. Skilling, in *Maximum Entropy and Bayesian Methods: Dartmouth 1989,* edited by P. F. Fougere (Kluwer, Amsterdam, 1990), p. 341.
[60] J. Skilling, in *Neutron Scattering Data Analysis 1990,* edited by M. W. Johnson (Institute of Physics, Bristol, 1990), p. 1.
[61] J. Skilling and R. K. Bryan, Mon. Not. R. Astron. Soc. **211**, 111 (1984).
[62] J. Skilling (private communication).
[63] P.-G. de Gennes, *Scaling Concepts in Polymer Physics* (Cornell University, Ithaca, 1979).
[64] F. Bruder and R. Brenn, Macromolecules **24**, 5552 (1991).
[65] P. F. Green and B. L. Doyle, Phys. Rev. Lett. **57**, 2407 (1986).
[66] M. Geoghegan, R. A. L. Jones, M. G. D. van der Grinten, and A. S. Clough (unpublished).
[67] T. G. Fox, Bull. Am. Phys. Soc. **1**, 123 (1956).
[68] M. Doi and S. F. Edwards, *The Theory of Polymer Dynamics* (Oxford University, Oxford, 1986).
[69] We estimate the reptation time from the ratio $\tau_{rep} \approx R_g^2/D^*$ using a value of D^*, the *d*-PS tracer diffusion coefficient, of $\sim 10^{-13}$ $cm^2 s^{-1}$ obtained from interdiffusion coefficient measurements on this blend [66]. Direct measurements of D^* on different *d*-PS–PαMS blends [70] further corroborate this result.
[70] M. G. D. van der Grinten, A. S. Clough, T. E. Shearmur, D. W. Drew, M. Geoghegan, and R. A. L. Jones (unpublished).
[71] G. Krausch, Mater. Sci. Eng. Rep. R **14**, 1 (1995).

[72] G. H. Fredrickson, in *Physics of Polymer Surfaces and Interfaces,* edited by I. C. Sanchez (Butterworth-Heinemann, Boston, 1992), p. 1.

[73] M. Geoghegan, R. A. L. Jones, A. S. Clough, and J. Penfold, J. Polym. Sci. B **33**, 1307 (1995).

[74] R. Lipowsky and D. A. Huse, Phys. Rev. Lett. **57**, 353 (1986).

[75] We have approximated the concentration gradient to $[\phi_m - \phi_d(z^*)]/(2\sqrt{Dt})$. This is equivalent to replacing the depletion layer depicted in Fig. 12 by a uniform gradient decreasing linearly to ϕ_d from ϕ_m over a length $2\sqrt{Dt}$. The factor of 2 is necessary for conservation of material.

[76] S. M. Troian, Phys. Rev. Lett. **71**, 1399 (1993). In this article the domains considered are rich in the nonwetting phase. There is no reason, however, to suppose that such anisotropic domains do not exist in our experiments, nor that they do not affect the growth of the wetting layer.

[77] M. Geoghegan, R. A. L. Jones, and A. S. Clough, J. Chem. Phys. **103**, 2719 (1995).